Supplementary Material

Description of the conventional DOAS system used for comparison in this study

A conventional, zenith-facing mobile DOAS system was integrated into the Cessna Conquest aircraft and used for comparison to the Imaging DOAS data presented in this study. Mounted directly adjacent to the Imaging DOAS entrance optics, a telescope containing a 20 mm-diameter fused silica lens with a focal length of 40 mm was used to couple downwelling UV radiance into a single 1 mm-diameter fused silica fiber. A Hoya U330 UV bandpass filter installed in the telescope blocked visible and infrared radiation at wavelengths longer than 430 nm from entering the spectrometer. The optical fiber was passed through a small hole in the aircraft fuselage and attached to the optical port of an Ocean Optics QE65000 research-grade spectrometer. This spectrometer features a back-thinned CCD detector that achieves high sensitivity in the UV spectral region. The detector was cooled to -10 degrees Celsius to reduce the CCD dark current. The spectrometer was placed in an insulated enclosure. The air temperature inside the enclosure was actively stabilized to 22 degrees Celsius to avoid variations in wavelength calibration or instrument line shape stemming from thermal expansion or contraction of the spectrometer's optical bench. Spectra were acquired using a laptop computer connected to the spectrometer's USB interface. The exposure time of individual acquisitions was adjusted to the illumination conditions such that the brightest pixel in the spectrum registered between 50 and 90 % of the detector's full dynamic range.

Analysis of the conventional DOAS spectra was performed using the same combination of MATLAB code (mDOAS) and the DOASIS software (Kraus, 2004)[1] and followed the same standard procedures as outlined for the Imaging DOAS and described in detail by Platt and Stutz (2008)[2]. See the "Spectral Retrieval" section of the main manuscript for additional details.

Any use of trade, product, or firm names is for descriptive purposes only and does not imply endorsement by the U.S. Government.

[1] Kraus, S. (2006). DOASIS - A Framework Design for DOAS. Dissertation, University of Mannheim. https://www.shaker.eu/en/content/catalogue/index.asp?lang=en&ID=8&ISBN=978-3-8322-5452-0.

[2] Platt, U., and Stutz, J. (2008). Differential Optical Absorption Spectroscopy - Principles and Applications. Berlin, Heidelberg: Springer doi:10.1007/978-3-540-75776-4.

Supplementary Table 1 – Radiative transfer model parameters used to simulate air mass factors (AMFs) for zenith and nadir-facing DOAS observations of volcanic SO_2 plumes (see Figure 7). All simulations were run with the 3D Monte Carlo atmospheric radiative transfer model McArtim (Deutschmann et al., 2011).†

Atmosphere	
Background	Pure Rayleigh atmosphere
Plume Shape	Cylindrical, extending to infinity along axis
Plume Diameter	500 m
Plume Altitude	500 – 4000 m (variable)
SO_2 Vertical Column Density	2.5×10^{17} molecules/cm^2
Plume Aerosol Optical Depth	0.1
Plume Single Scatter Albedo	0.9
Scattering Phase Function	Henyey-Greenstein
Scattering Asymmetry Parameter	0.8
Instrument	
Position	Centered over/under plume
Altitude	250 – 4250 m (variable)
Field of View	Circular, 0.5 degree aperture
Elevation Angle	90 (zenith-facing), -90 (nadir-facing) (variable)
Raytracing	
Solar Zenith Angle	40 degrees
Solar Azimuth Angle	Perpendicular or parallel to plume (variable)
Wavelength	313 nm
Number of Simulated Photons	10^5
Ground Albedo	0.06, 0.8 (variable)

† Deutschmann, T., Beirle, S., Frieß, U., Grzegorski, M., Kern, C., Kritten, L., Platt, U., Prados Román, C., Puķite, J., Wagner, T., Werner, B., Pfeilsticker, K. (2011) The Monte Carlo atmospheric radiative transfer model McArtim: Introduction and validation of Jacobians and 3D features. *J. Quant. Spectrosc. Radiat. Transf.* 112, 1119–1137. doi:10.1016/j.jqsrt.2010.12.009.

A

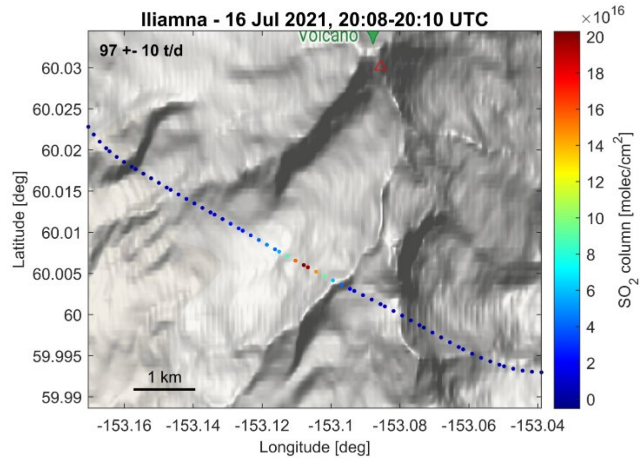

B

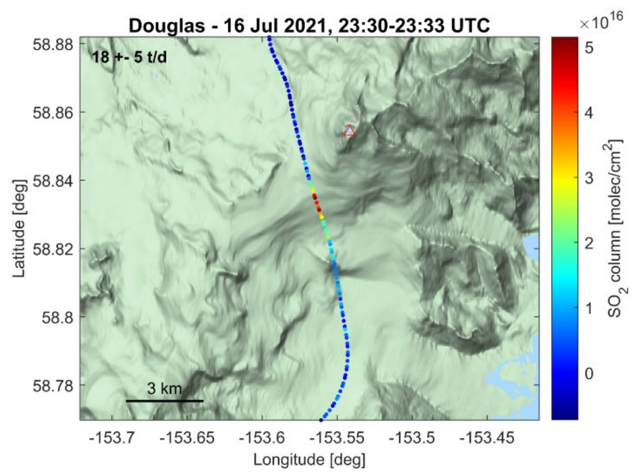

C

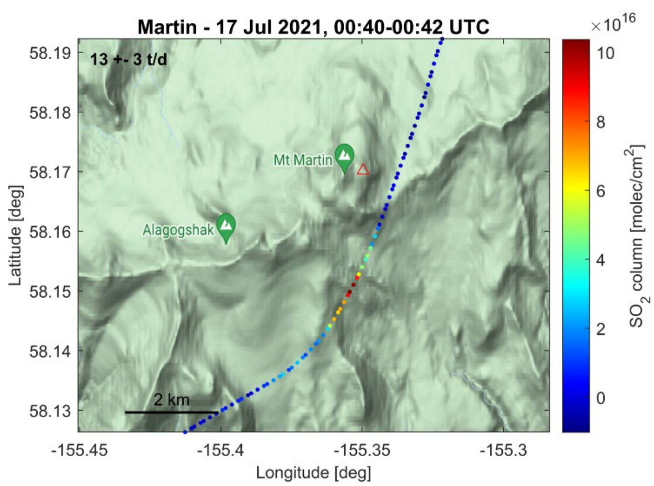

Supplementary Figure 1 – Example measurements of the SO_2 emission rate from (A) Iliamna Volcano, (B) Mount Douglas, and (C) Mount Martin performed with the conventional DOAS system installed on the Cessna Conquest aircraft. This system is based on an Ocean Optics QE65000 spectrometer and achieves a higher signal-to-noise ratio than each individual viewing direction of the Imaging DOAS (see Figure 6) but lacks the spatial information provided by the imaging system. Note that final emission rates were compiled from multiple plume traverses at each volcano, not just from the examples shown here.

A

B

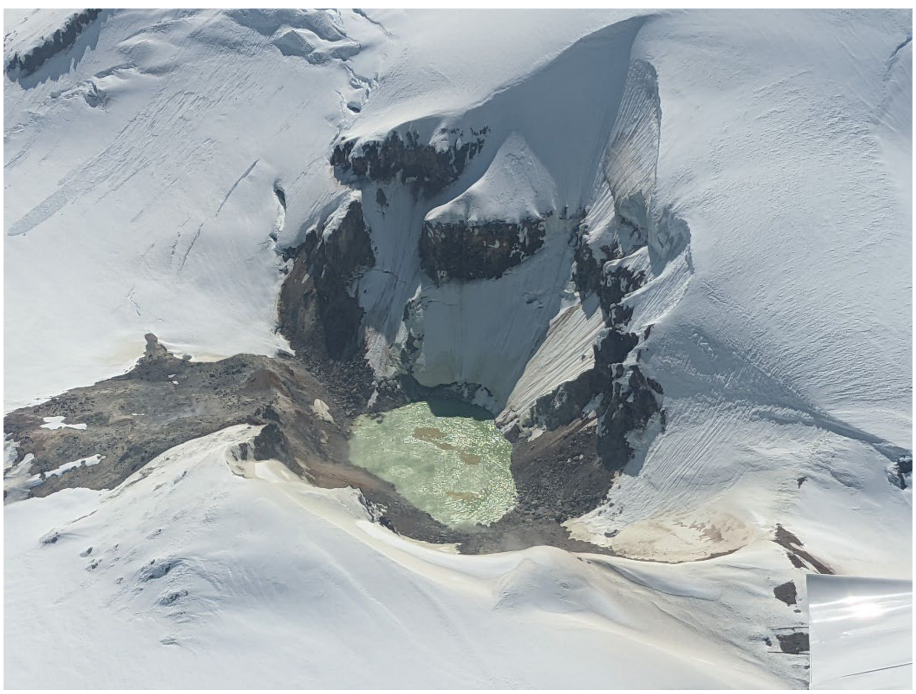

Supplementary Figure 2 – (A) Mount Mageik's phreatic crater viewed from the south-southeast. The volcano's central cone extends off the image to the left, while its north cone is fully captured in the background. (B) Viewed from the east, the phreatic crater contains an acidic crater lake. During our overflight, large bubbles repeatedly breached the lake surface in the southeast quadrant (bottom left in the image), and a brown raft of what appeared to be sulfur spherules floated on the lake. Photos by Christoph Kern, USGS.

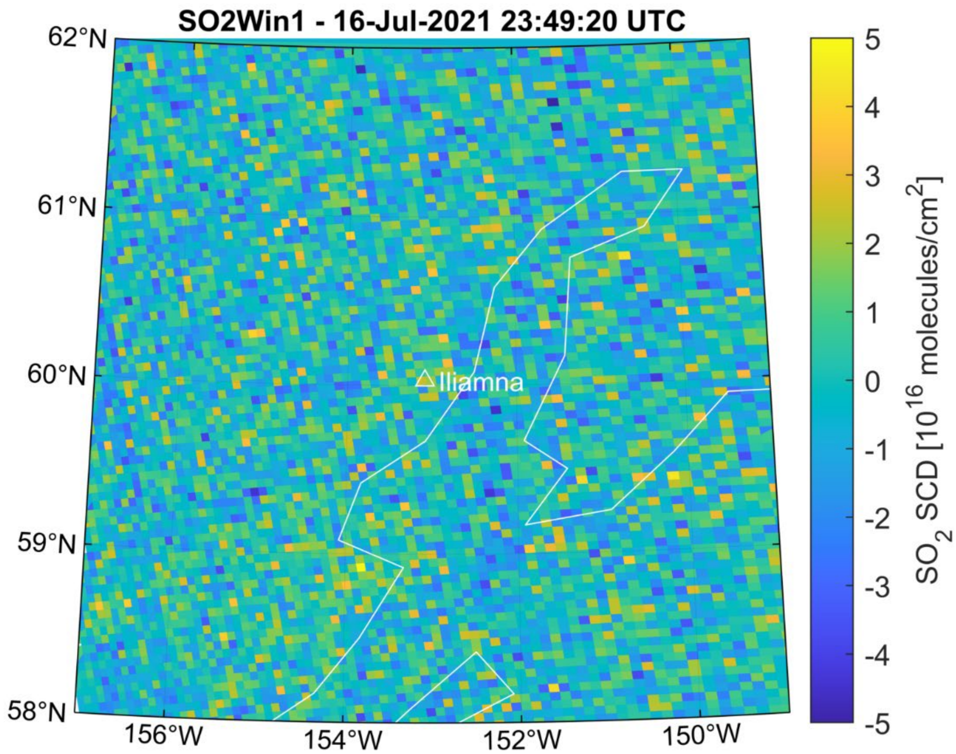

Supplementary Figure 3 – Sulfur dioxide (SO_2) slant column density (SCD) measured by the Tropospheric Monitoring Instrument (TROPOMI) on board the Copernicus Sentinel-5 Precursor satellite over the Cook Inlet, Alaska (white coastline), on 16 July 2021 at 23:49 UTC. The shown SCDs were retrieved in fit window 1 (312-326 nm) and provided in the S5P Offline SO_2 product (ver. 02.02.01 from 19 July 2021). SO_2 is not enhanced above the noise level at the location of Iliamna Volcano (indicated by a triangle in the image). Downloaded on 29 September 2022 from the Sentinel-5 Precursor Open Access Data Hub: https://s5phub.copernicus.eu/dhus/#/home